

Measuring the Hall Effect and Characterizing a Helium Glow Discharge

Ian Haines

*Physics Department, University of California, Berkeley
366 Physics North, Berkeley, CA 94720*

Low density plasma provides the opportunity to observe a large, measurable Hall voltage. As a result, these low-density plasmas are easy to characterize. Using a simple apparatus, one of these plasmas was created and the Hall voltage as a function of an external magnetic field, discharge voltage, and pressure was measured. From these measurements, the electron drift velocity and density were deduced. Combined with a measurement of the plasma resistivity, the electron collision frequency was also deduced. The electron temperature was then estimated from these values. Included are the results and an analysis of the errors.

I. INTRODUCTION

Irving Langmuir did not set out to create a new sub-field of physics, but he did just that in his study of ionized gases in the 1920's. He gave the name "plasma", derived from the ancient Greek $\pi\lambda\alpha\sigma\mu\alpha$ meaning "jelly", to this ionized gas. Since Langmuir's initial discovery, plasma has been recognized as a fourth fundamental state of matter alongside solid, liquid, and gas. Physicists have not only created various types of plasma within the laboratory setting, but they have also found them naturally occurring such as in stars and other astrophysical objects [1]. Most recently, much research within plasma physics has been focused in harnessing extremely high density, high temperature plasma, like that found in stellar cores, to produce large-scale sustainable energy [2]. However, many of the properties of plasma are still unknown such as how it transitions from the gas phase to the plasma phase [3]. Hence, further studies are needed to better understand both naturally occurring and man-made plasma.

In this experiment, we set out to characterize a low-density column discharge using a He gas mixture. In a low-density plasma such as the one we created, the Hall effect is large and observable. This allowed for the properties of the discharge to be characterized easily.

II. SIMPLE THEORY OF PLASMA

Before describing the theoretical features of glow discharges, it is important to develop a general theory of plasma. Plasma can be understood through the applications of rudimentary mechanics, electrodynamics, and statistical physics. Specifically, the applications of Newton's laws, the Lorentz force law, and Boltzmann statistics. The following development will mirror that of [4]. For further details and discussion, we refer to that paper.

A. Ohmic Properties of Plasma

A plasma can be thought of as a conducting, ionized gas so that both free electrons and ions are moving and colliding with each other like in a conductor. In a typical conductor with one species of charge carrier, there is an associated carrier charge, q , charge carrier density, n_q , and charge carrier mass, m_q . If the charge carriers move with a drift velocity, \mathbf{u}_q , then the current density is

$$\mathbf{j} = qn_q \mathbf{u}_q. \quad (1)$$

This drift velocity is not the velocity of a single charge carrier but the expectation value of the velocity of each carrier in the gas

$$\mathbf{u}_q = \langle \mathbf{u} \rangle. \quad (2)$$

By applying a strong enough discharge field, \mathbf{E}_d , to the gas, it can become ionized. Thus, Ohm's law states

$$\mathbf{E}_d = \eta \mathbf{j}, \quad (3)$$

where η is the resistivity of the plasma. This resistivity is due to collisions between the carriers and themselves or with the ions. Hence, this frictional force takes the form

$$\mathbf{F}_f = -m_q \nu_q \mathbf{u}_q, \quad (4)$$

where ν_q is the collision frequency or momentum loss frequency. Since the current is steady in the plasma, the force from the electric field must be equal to the frictional force. Newton's second law states

$$q\eta \mathbf{j} - m_q \nu_q \mathbf{u}_q = 0, \quad (5)$$

and so eq's 1 and 5 give

$$\eta = \frac{m_q \nu_q}{q^2 n_q}. \quad (6)$$

B. The Hall Effect

Every physics student encounters the Hall effect at some point early in their physics education. It is simply the phenomenon whereby a potential difference is

generated across a conducting material via an external magnetic field and orthogonal to the direction of propagation (see Fig 1). In this development, the geometry of the tube is assumed to be that of a plane slab. If the mean free path of the particles is small, then the global geometry looks like the local plane slab geometry. So, this is a good approximation.

The effect can be understood by applying the Lorentz force law. The law states

$$\mathbf{F} = q(\mathbf{E} + \mathbf{u}_q \times \mathbf{B}). \quad (7)$$

where $\mathbf{E} = \mathbf{E}_d + \mathbf{E}_H$. Applying Newton's second law again yields, as can be seen in Fig. 1,

$$\mathbf{E}_H = -q\mathbf{u}_q \times \mathbf{B} = \frac{1}{n_q} \mathbf{B} \times \mathbf{j}. \quad (8)$$

What separates a discharge column and solid conductors is that the number density of charge carriers in the discharge column is significantly smaller than the number density in solid conductors. Equation 8 shows that the Hall field and voltage is much greater in the discharge column. So, the Hall voltage can be measured much more easily in this experimental setup.

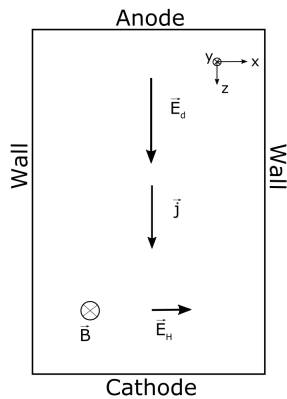


FIG. 1. Plane slab geometry slice of the glow discharge column ignoring the pressure gradient. The Hall voltage can be measured across the x-direction due to \mathbf{B} in the y-direction and the drift velocity in the z-direction.

Although eq 6 was shown without the added external \mathbf{B} field, it will be seen in the results that the Hall field is roughly 1 order of magnitude smaller than the discharge field, so the equation is a good first order approximation.

C. Glow Discharge: the Pressure Gradient

Although charges collide with ions, recombination doesn't happen except at the walls of the tube. The reason for this is a pressure gradient that decays from a maximum value at the center to zero at the walls. This

gradient can be understood through the "temperature" of the electrons. This temperature couples the density of the charge carriers to the electric field. Newton's second law gives

$$qn_q \mathbf{E} + qn_q \mathbf{u}_q \times \mathbf{B} - qm_q \nu_q \mathbf{u}_q - \nabla(n_q k_B T_q) = 0 \quad (9)$$

where $\mathbf{E} = \mathbf{E}_d + \mathbf{E}_H + \mathbf{E}_p$. Important to note is the addition of the charge carrier density to the coefficients of each term. The force balance equation treats the entire collection of particles, thus yielding

$$\mathbf{E}_p = -\frac{\nabla(n_q k_B T_q)}{qn_q}. \quad (10)$$

This field is generated through the anisotropic charge distribution generated in the plasma's creation. As soon as the charge begins to accumulate in one region of space, this pressure gradient is simultaneously created to counteract the further accumulation of charge. Thus, this gradient can be understood as a field transmitting information to surrounding charges so that they stay combined with their ions. This forces what is called "quasineutrality" which can be represented algebraically as

$$n_q = n_i \quad (11)$$

where n_i is the number density of the ions.

It is a reasonable assumption that the thermal energy of each charge carrier is roughly equal across the width of the tube and so the force becomes

$$\mathbf{F}_p = -k_B T_q \nabla \ln n_q \quad (12)$$

The force balance equation, eq. 9, is a vector differential equation. However, the y- and z-coordinates vanish for each vector leaving an ordinary differential equation in the x-coordinate

$$n_q E_x + n_q u_{qx} B + \frac{m_q \nu_q}{q} n_q u_{qx} + \frac{k_B T_q}{q} \frac{dn_q}{dx} = 0. \quad (13)$$

It is important to note that the pressure gradient creates a small drift velocity u_{qx} in the x-direction. Yet, there cannot be current flowing in that direction else there would be a charge build-up at the walls of the tube. Hence, there must also be an ion drift velocity u_{ix} and $n_q u_{qx} = n_i u_{ix}$. Quasineutrality then forces $u_{qx} = u_{ix}$. This kind of charge flow is called "ambipolar", and the pressure gradient field will adjust itself until it reaches "ambipolarity".

D. Measuring the Hall Voltage

Since the current in the plasma is steady, any recombination that happens at the walls must be counterbalanced by ionization within the plasma. This continuity relation is expressed algebraically as

$$\frac{d}{dx}(n_i u_{ix}) = \frac{d}{dx}(n_q u_{qx}) = \nu^i n_q \quad (14)$$

where ν^i is the frequency of ionization and is dependent upon T_q .

Related to the charge equation of motion (eom), equation 9, is the ion eom. Because $m_i = m_{gas} \gg m_q$, $u_{ix} \ll u_{qx}$ via conservation of momentum. Moreover, due to conservation of energy, $T_i \approx T_g \ll T_q$. This means the Hall and pressure terms essentially vanish for the ions. Thus, the ion eom reduces to

$$\mathbf{E} - \frac{m_i \nu_i}{q} \mathbf{u}_i = 0. \quad (15)$$

The quasineutrality and continuity relations along with equation 13 and the ion eom give the charge eom:

$$\frac{d^2 n_q}{dx^2} + a \frac{dn_q}{dx} + bn_q = 0 \quad (16)$$

where

$$a = -\frac{e E_H}{k_B T_q} \quad (17)$$

$$b = \frac{m_q \nu_i \nu^i}{k_B T_q}. \quad (18)$$

This differential equation will be recognized as that for an RLC circuit whose solutions are damped, harmonic oscillations. This gives rise to the charge distributions as seen in Fig. 2. The solutions to 16 have the form

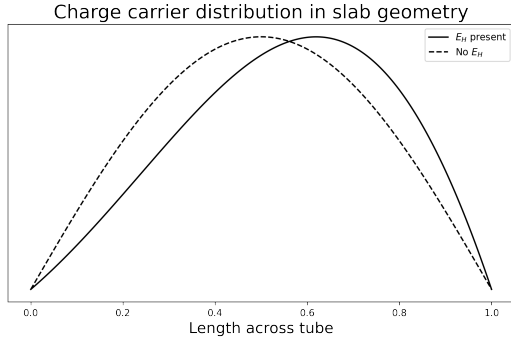


FIG. 2. Charge carrier distributions across the length of the tube. The symmetric distribution is without the magnetic field generating the Hall voltage. The asymmetric distribution is a non-equilibrium distribution that results in the observed Hall effect.

$$n_q(x) = n_0 \exp\left(-\frac{ax}{2}\right) \sin\left(\frac{x}{\Lambda}\right) \quad (19)$$

where $\Lambda = b = \frac{\pi^2}{L^2}$ is known as the diffusion length. Note that if $E_H = 0$, then $a = 0$ and the skewed distribution in Fig. 2 reduces to the symmetric one.

Using equation 15, E_x can be solved for in equation 19. Integrating over some distance $\Delta x = x_2 - x_1$ gives

the Hall voltage:

$$\Delta\phi(x_1, x_2) = \int_{x_1}^{x_2} E_x dx \quad (20)$$

$$= \frac{\Delta x}{2} E_H - \frac{k_B T_q}{q} \ln \left[\frac{\sin(\pi x_2/L)}{\sin(\pi x_1/L)} \right] \quad (21)$$

It is apparent that the Hall voltage is more complicated than just the change in the distance multiplied by the field strength. Rather, there is an extra term introduced that depends upon the distribution of the charges due to the temperature. Also interesting to note is that if the distance from x_1 and x_2 to $L/2$ are both equal, then the second term vanishes. This is due to the ambipolar characteristic of the field which causes the diffusion rates of the ions and charges to be equal. As a result, only half of the Hall field is observed.

III. CHARACTERIZING THE PLASMA

Using a measurement of the discharge current, I_d , and the cross-sectional area of the tube, the current density, \mathbf{j} , can be found. Using equations 1 and 8, n_q and \mathbf{u}_q can be found. These values along with the discharge and Hall voltages can be used to determine ν_q from equation 7:

$$\nu_q = \frac{E_d q B}{E_H m_q} = \frac{E_d}{E_H} \Omega_q \quad (22)$$

where Ω_q is the cyclotron frequency of the charges.

Once ν_q is known, the resistivity of the plasma can be determined from equation 6. Similarly, the collision frequency is related to the density of the gas, the scattering cross-section, and the drift velocity of the charges:

$$\nu_q = n_{gas} \langle \sigma v \rangle_q \quad (23)$$

where the number density of the gas is simply given by the ideal gas law. In the general case, σ has a dependence upon the velocity of the charge carrier. The energy range at which the apparatus operates at is low enough that $\sigma(v) \approx \sigma \approx 5 \times 10^{-20} \text{ m}^2$. Hence,

$$\langle v \rangle_q \approx \frac{\nu_q}{p \sigma (3 \times 10^{22})} \frac{T_g}{273} \quad (24)$$

where T_g is the gas temperature and p is measured pressure.

IV. APPARATUS AND PROCEDURE

A. Experimental Design

Modularity is the driving principle behind the apparatus used, for it must be able to apply different fields and produce measurements for various quantities. The

apparatus was designed with this idea in mind, and its actual components can be broken down simply. A detailed schematic can be found in Fig. 3 (reproduced from [4]).

First, a gas source that will ionize at low pressure and a potential difference of ~ 3000 V and a current of ~ 3 mA is needed. A 98.9% He, 1% Ar, and 0.1% N₂ gas mixture was used. The gas source was connected to a discharge tube which connected to a vacuum pump on the other side. This allowed for the pressure to be controlled finely through different gauges and valves. This setup creates the low-pressure gas flow through the tube which is ionized to create the plasma.

The next aspect of the apparatus is the high voltage source that generates the discharge voltage and thus the discharge current. This voltage source has a range of 0 – 3000 V and a current range of 0 – 3 mA. The gas enters at the anode and exits at the cathode; the distance between the cathode and anode is ~ 75 mm. Depending on the pressure in the tube, the necessary potential difference across the gas will differ. As the pressure increases, a higher potential difference is needed to ionize the gas. This can be explained by the fact that at higher pressures, the density of the gas will be greater. As a result, the mean free path is shorter so that electrons cannot stay ionized for long, so they recombine immediately.

In addition to the circuitry applying the potential difference, there is another subcircuit which applies the external magnetic field. This field is generated using a solenoidal geometry. The current running through the solenoid has a range of -2.5 – 2.5 A. This generated a magnetic field with a field strength of roughly -750 – 650 gauss.

To make measurements, a set of probes were placed in select spots along the longitude of the discharge tube. One set of probes was used to display I_d in the plasma on an oscilloscope. This will be explained in more detail in the succeeding section on oscillations and striations. Another set of probes was used to measure the Hall voltage when the plasma was subjected to the external magnetic field. This set of probes achieved the results seen in equations 20 and 21.

V. INSTABILITIES, OSCILLATIONS, AND STRIATIONS

A stable plasma can be seen in Fig. 4. In this case, the plasma is uniform and has continuous translational symmetry along the longitudinal direction. On the oscilloscope, there may be some oscillations in the current. However, the peak-to-peak amplitude will be smaller than 50 mV.

Conversely, an unstable plasma can be seen in Fig. 5. This plasma is clearly different from the stable plasma. In the unstable plasma, the symmetry is broken. Instead, it is rarefied. This rarefaction phenomenon is known as a striation. These striations arise due to the distance be-

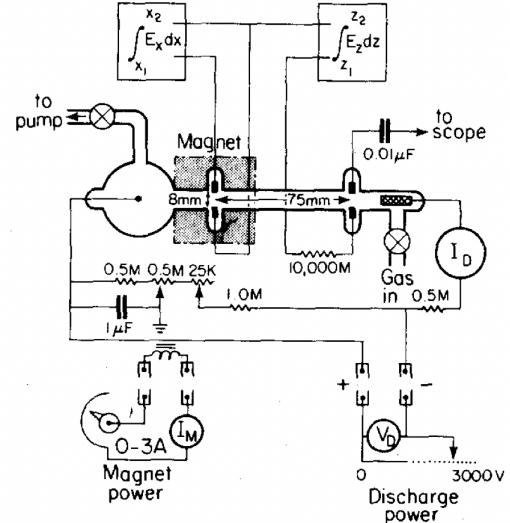


FIG. 3. Schematic of the apparatus used to measure the Hall voltage in the glow discharge.

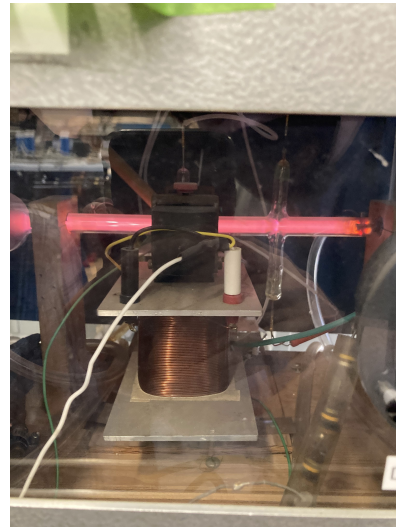


FIG. 4. Stable glow discharge.

tween the probes that create the discharge potential difference. As a result, these striations will also depend on the potential difference itself and the pressure in the tube. This phenomenon is an indication of an unstable plasma. This is unwanted when taking measurements and characterizing the quantities of the plasma. This instability can also be seen on the oscilloscope where the peak-to-peak voltage will be > 50 mV and will jump around.

VI. MEASUREMENTS

Using the apparatus as described above, a few types of data were measured and under different conditions.



FIG. 5. Unstable, striated glow discharge.

A. Discharge Current and Voltage

In the first set of measurements taken, the plasma was generated at a variety of pressures in the range of 15 – 30 torr. The reason for this measurement was to get an understanding of the relation between I_d and V_d . From V_d , E_d was obtained. This was necessary to carry out calculations used to determine the quantities of interest. We found ohmic fields in the range of roughly $\sim 1500 \text{ V} \cdot \text{m}^{-1}$ (see Table I). See figures 8 through 14.

B. Magnetic Current and Field Strength

The next set of measurements were those of the relation between the current of the solenoidal electromagnet and the measured magnetic field. The magnetic field was measured using an external Gauss meter while the current was measured via a gauge readout on the apparatus itself. This was performed to see any potential hysteretic effects (see Fig 6).

C. Hall Voltage and Magnetic Field Strength

The final measurement performed was the Hall field strength versus the magnetic field strength. This measurement was performed numerous times over a range of pressures from 15 – 30 torr. From these measurements, the other quantities of interest could be determined. See figures 15 through 21.

The discharge voltage was constant for each high voltage value. However, it did change for each pressure value leading to the plot below.

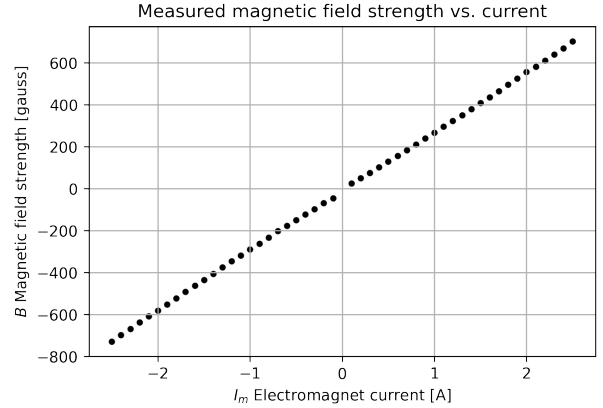


FIG. 6. Magnetic field strength in both the forward and reverse current regimes. The plot is quite clearly linear for both small and large currents. We can conclude that any hysteresis present is negligible.

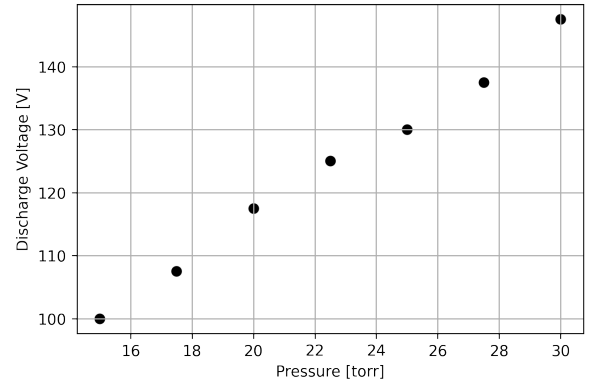


FIG. 7. Discharge voltage measured at each pressure value

VII. CALCULATIONS AND ERROR ANALYSIS

From the measurements described in the previous sections, we were able to characterize the plasma by calculating 8 parameters: the mean electron temperature, T_e , the mean electron energy, E_e , the mean collision rate, ν_e , the drift velocity, u_e , the mean electron density, n_e , the mean ionization degree, i , the mean velocity in the gas frame, v_e , and the mean resistivity, η . We have calculations for 15 torr, 17.5 torr, 20 torr, 22.5 torr, 25 torr, 27.5 torr, and 30 torr. We only used the values for both the Hall and magnetic fields where the magnetic field was less than 300 gauss because this regime was the most linear.

A. Collision Frequency

First, we calculated the collision frequency by using equation 22. The values for each pressure all fell within one order of magnitude of each other (see Fig. 22). There

Pressure [torr]	15 ± 0.1	17.5 ± 0.1	20 ± 0.1	22.5 ± 0.1	25 ± 0.1	27.5 ± 0.1	30 ± 0.1
E_d [V/m]	1333 ± 30	1433 ± 30	1566 ± 30	1666 ± 30	1733 ± 30	1833 ± 30	1966 ± 30

TABLE I. Ohmic or discharge field as a function of discharge tube pressure. The uncertainties are due to measuring numbers from analog gauges.

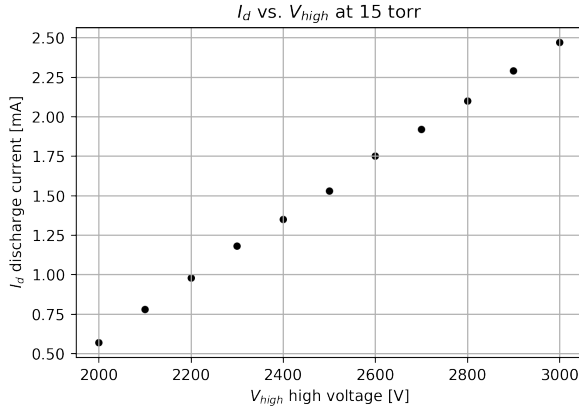


FIG. 8. High voltage-discharge current characteristic curve at 15 torr.

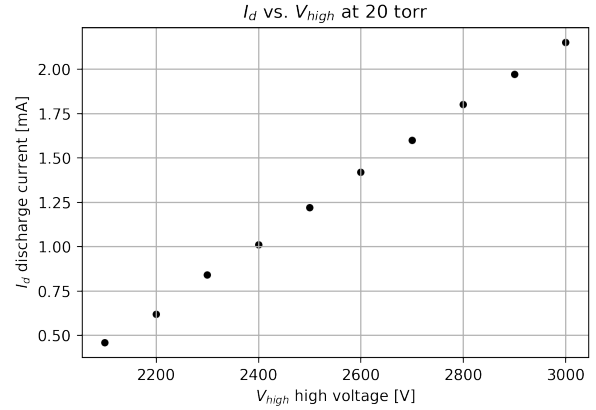


FIG. 10. High voltage-discharge current characteristic curve at 20 torr.

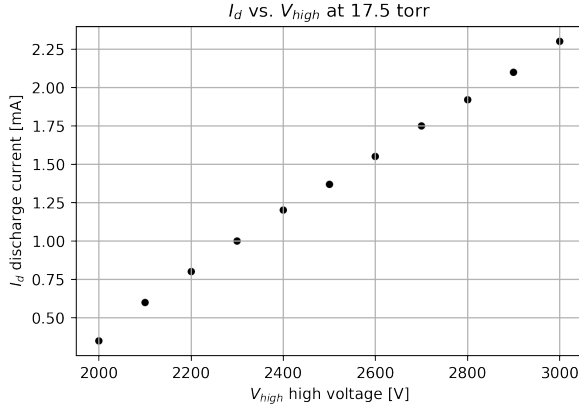


FIG. 9. High voltage-discharge current characteristic curve at 17.5 torr.

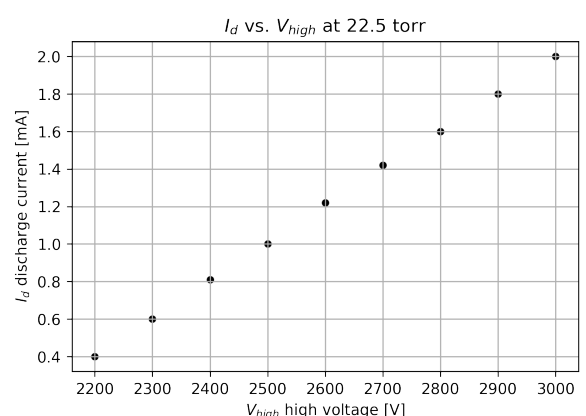


FIG. 11. High voltage-discharge current characteristic curve at 22.5 torr.

is no apparent trend visible from the data, and the errors are quite large making any determination of a trend line a useless endeavour. It can be said that the value should be roughly 1×10^{10} collisions per second.

1. Errors

The errors were calculated using an error propagation method. This gives the formula

$$\sigma_\nu = \nu \sqrt{\left(\frac{\sigma_d}{E_d}\right)^2 + \left(\frac{\sigma_H}{E_H}\right)^2 + \left(\frac{\sigma_B}{B}\right)^2} \quad (25)$$

All of these sources of error could have contributed. However, the magnetic field uncertainty is less likely to contribute to the observed errors. The reason for this is that the magnetic field did not vary much over the course of the period the experiment was conducted. Additionally, the magnetometer was zeroed before each set of measurements was recorded. The discharge voltage could potentially vary quite a lot. The reason for this is that sometimes the plasma would become unstable and disappear. If the gas has to be re-ionized, it is possible that it does not have the same characteristics as before. It is also possible that the impurities of the gas could affect the measurements as well. However, these impurities

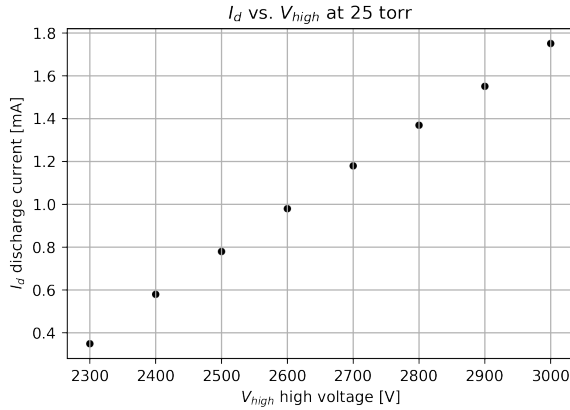


FIG. 12. High voltage-discharge current characteristic curve at 25 torr.

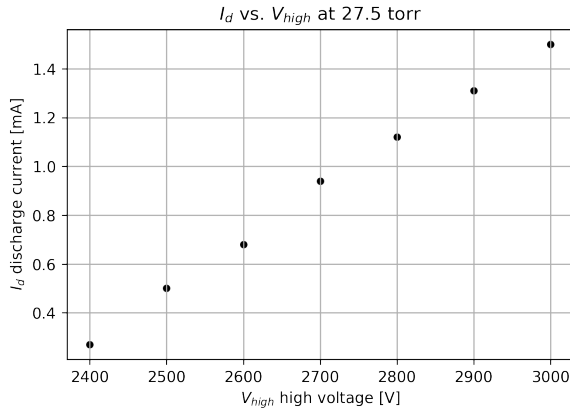


FIG. 13. High voltage-discharge current characteristic curve at 27.5 torr.

would be a systematic error.

B. Drift Velocity

The drift velocity was calculated using equations 3 and 5 (see Fig. 23). In this case, the drift velocity at 15 torr is an outlier.

1. Errors

The errors for the drift velocity were calculated using the following formula:

$$\sigma_u = u_e \sqrt{\left(\frac{\sigma_H}{E_H}\right)^2 + \left(\frac{\sigma_B}{B}\right)^2} \quad (26)$$

For the drift velocity, the magnetic field uncertainty is, again, less likely to affect the uncertainty calculation.

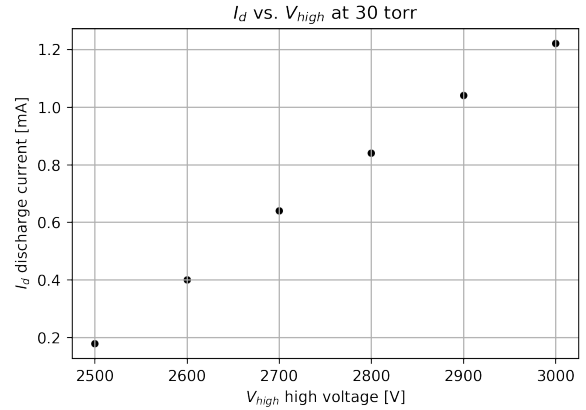


FIG. 14. High voltage-discharge current characteristic curve at 30 torr.

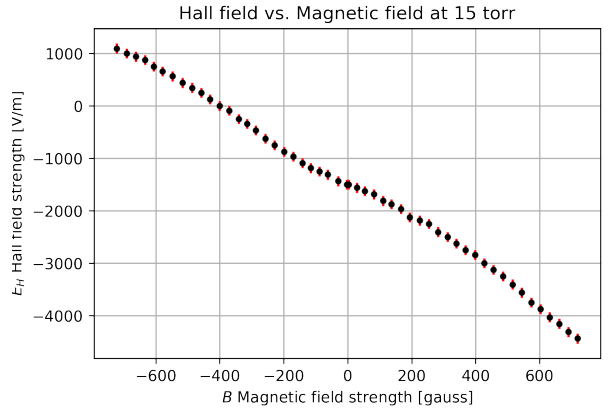


FIG. 15. Hall field strength versus magnetic field strength at 15 torr.

The Hall field at 15 torr is not entirely linear in the magnetic field strength regime used. This could potentially be causing the large value observed at 15 torr. Despite the fact that this value is larger, values are only expected to be correct within one order of magnitude. Plasma physics is inherently lacking in the precision of that seen in atomic spectroscopy.

C. Electron Density

The electron density was obtained from equations 3 and 5 (see Fig. 24). Again, these values are all within roughly one order of magnitude of each other. Additionally, the values decrease with increasing pressure which is expected. As the pressure increases, a greater force is needed to ionize the electrons from the Helium. Hence, there should be less free electrons if the force is the same at each pressure.

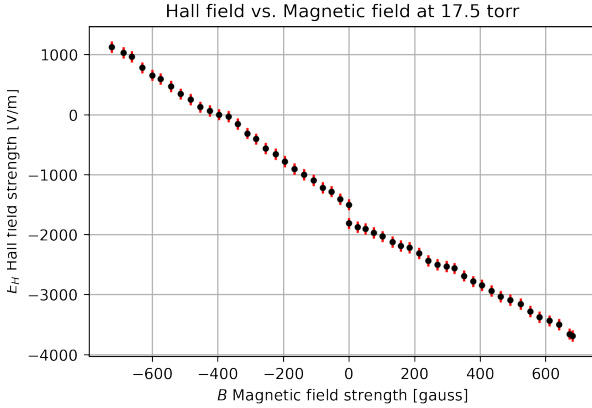


FIG. 16. Hall field strength versus magnetic field strength at 17.5 torr.

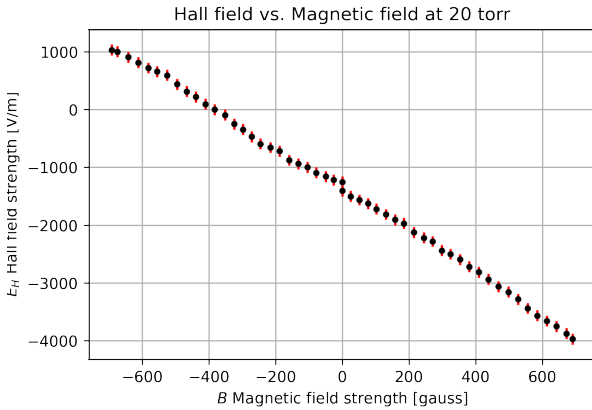


FIG. 17. Hall field strength versus magnetic field strength at 20 torr.

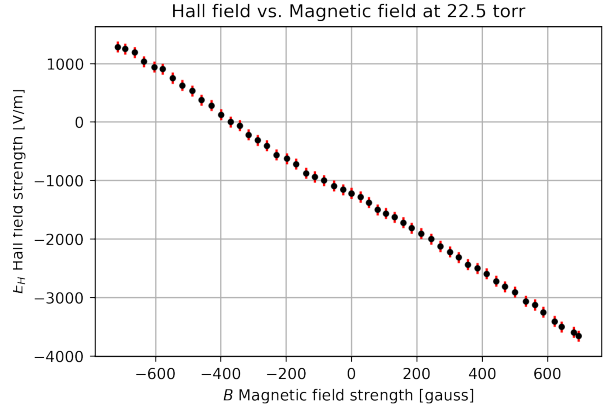


FIG. 18. Hall field strength versus magnetic field strength at 22.5 torr.

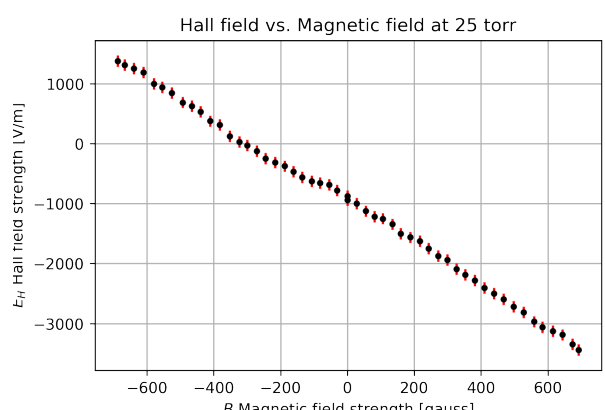


FIG. 19. Hall field strength versus magnetic field strength at 25 torr.

1. Errors

The error propagation formula for the electron density is given by:

$$\sigma_{n_e} = n_e \sqrt{\left(\frac{\sigma_j}{j}\right)^2 + \left(\frac{\sigma_u}{u_e}\right)^2} \quad (27)$$

The errors are quite large due to the errors in the drift velocity being quite large themselves. However, although the variation seems large, they are within one order of magnitude. Again, this is the level of accuracy expected within an experiment of this nature.

D. Ionization Fraction

The ionization fraction was calculated by taking the ratio between the electron density and the gas atom den-

sity:

$$i = \frac{n_e}{n_g} \quad (28)$$

where $n_g = 3 \times 10^{22} p$ where p is the pressure in torr (see Fig. 25) Similar to the electron density, there is a clear trend in which the higher pressure values see a lower degree of ionization. This is explained by the trend in the electron density.

1. Errors

The errors for the ionization fraction were calculated by using an error propagation method. This yielded relatively small errors that were all within an order of magnitude.

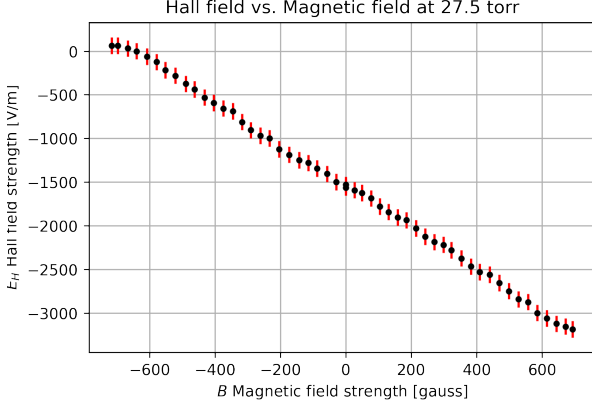


FIG. 20. Hall field strength versus magnetic field strength at 27.5 torr.

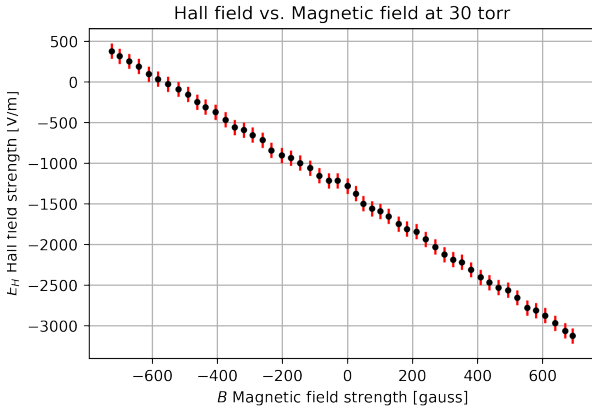


FIG. 21. Hall field strength versus magnetic field strength at 30 torr.

E. Velocity in the Gas Frame

The velocity of the electrons in the gas frame was calculated using equation 24. The gas temperature was set to room temperature and the scattering cross section was at a constant value. There isn't a clear trend in these values, but it appears to be roughly constant for each pressure value. This would appear to make sense considering the gas is moving at a greater velocity at higher pressure as well as the electrons and so the relative velocity should be roughly equal across each pressure (see Fig. 26).

1. Errors

The errors were calculated by propagating errors. The largest source of error in this calculation was the error in the collision frequency. The errors for the collision frequency are relatively large leading to relatively large errors for the velocity in the gas frame. However, the values are all within one order of magnitude.

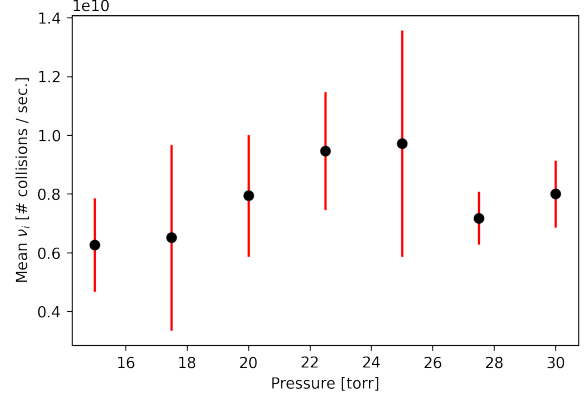


FIG. 22. Mean collision frequency at each pressure with given errors. Errors were calculated using error propagation techniques.

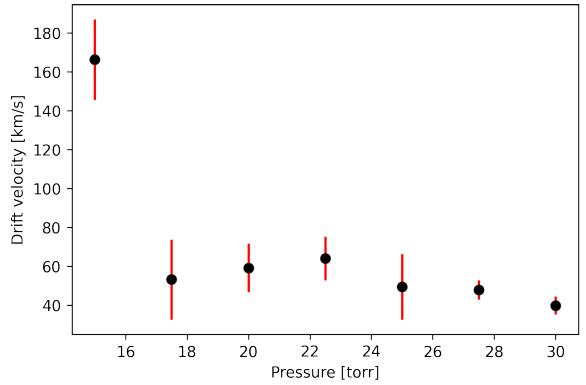


FIG. 23. Mean drift velocity for each pressure value. Error bars were calculated by an error propagation method.

F. Resistivity

The resistivity was calculated using equation 6. This calculation showed a clear scaling relation:

$$\eta \propto p$$

This scaling relation can be argued for due to the fact that

$$\eta \propto \frac{\nu_e}{n_e}.$$

Both ν_e and n_e scale as E_H/B . Thus, any errors in both of these terms will cancel out and so the calculations are robust (see Fig. 27).

1. Errors

The errors for η were calculated using error propagation. As stated before, the errors from both the Hall field

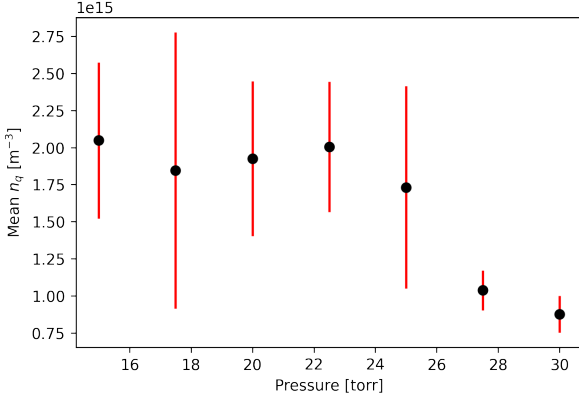


FIG. 24. Mean n_e at each pressure. The error bars were calculated using an error propagation formula.

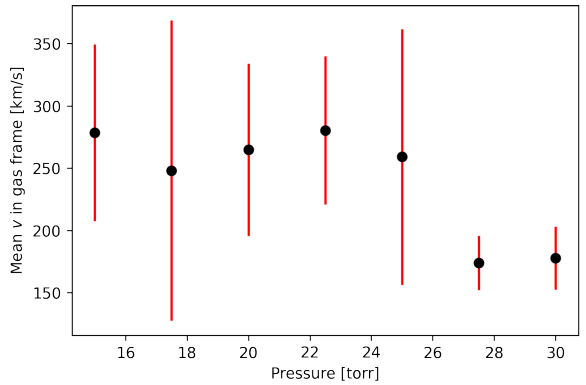


FIG. 26. Mean velocity in gas frame for each pressure value. Error bars were calculated via error propagation.

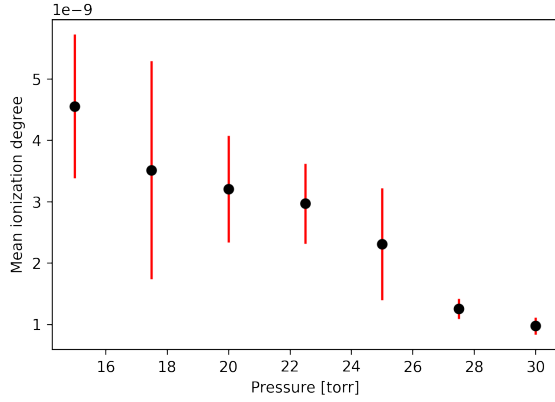


FIG. 25. Mean ionization fraction for each pressure value. The error bars were calculated via an error propagation method.

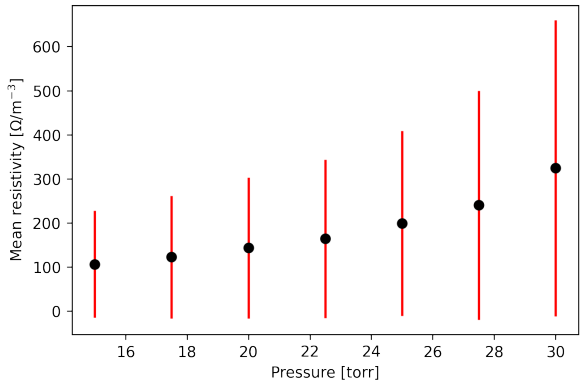


FIG. 27. Mean η values for each pressure. Error bars were calculated using error propagation.

and magnetic field cancelled out. Thus, the only sources of error are in the discharge field uncertainty and current density uncertainty at each pressure coming from the calculations for the collision frequency and electron density.

G. Energy

The energy was calculated using the kinetic energy formula where the velocity was the calculated drift velocity. These values don't show a trend yet they are all roughly within the range of ~ 1 eV and nearly constant (see Fig. 28).

1. Errors

The only source of error for the energy calculation is the uncertainty in the calculation for the drift velocity.

Because the energy has a squared dependence on the drift velocity, any errors are squared thus potentially leading to large errors in the energy. Despite this, all of the values for the energy, even within error, lie near ~ 1 eV.

H. Temperature

The electron temperature is found using the standard Kelvin to eV conversion: $1 \times 10^4 \text{ K} = 1 \text{ eV}$. Thus, the temperature different from the energy only by a constant value (see Fig. 29). Although the temperature values seem low despite ionization taking place, it must be understood that these are mean temperature values at each pressure and they are understood to be mean temperature values across the entire width of the tube. At the center of the tube, the electrons have a higher temperature due to ionization.

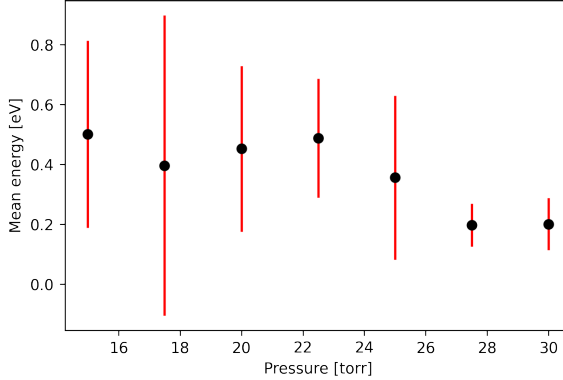


FIG. 28. Mean E values for each pressure. Error bars were calculated using error propagation.

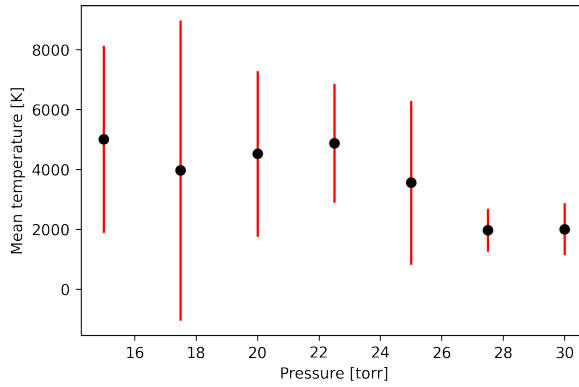


FIG. 29. Mean temperature value for each pressure point. The error bars were calculated using an error propagation technique.

1. Errors

The error analysis for the temperature mirrors that of the energy. Again, the values appear to be roughly

constant across the various pressures. Yet this cannot be concluded with certainty due to the large errors.

VIII. CONCLUSION

Plasma physics is a relatively new subfield of physics. Because of this, there are many unanswered questions within it. Additionally, plasma is inherently unstable making it difficult to study and characterize. A better understanding of plasma would advance not only our understanding of physics but also our ability in plasma physics applications such as in building fusion reactors for sustainable energy. With that being said, we can characterize simple types of plasma such as glow discharges. We can do this by using a simple theory that combines the principles of electrodynamics, thermal physics, and analytic mechanics. This is done by measuring the Hall effect which is large and observable for a plasma due to the low charge carrier density relative to a semiconductor. Using this approach, we found various scaling relationships for parameters such as the resistivity and the electron density at different pressures. We only expect these types of rough relationships due to the difficulty of stabilizing plasma. Further investigations into plasma are warranted.

Such investigations in the future should incorporate more intelligent ways to stabilize plasma so that they could be studied more rigorously. In this more rigorous setting, scaling relations could eventually become refined. Additionally, the theory could be better tested against experiment so that other effects that are not as widely apparent at such a simple level do manifest and can be observed.

ACKNOWLEDGMENTS

We would like to thank Rachel Wang for her patience and contributions to measuring various values. We would also like to thank Leander, Lukasz, Nathaniel, and Luc for all of their guidance in operating the apparatus used.

-
- [1] R. J. Goldston and P. H. Rutherford, *Introduction to plasma physics* (Institute of Physics Pub., 1997).
 - [2] World nuclear association, <https://web.archive.org/web/20150719060659/http://www.world-nuclear.org/info/current-and-future-generation/nuclear-fusion-power/>.
 - [3] A. I. Morozov, *Introduction to plasma dynamics* (Taylor & Francis, 2013).
 - [4] W. B. Kunkel, Hall effect in a plasma, *American Journal of Physics* **49**, 733 (1981), <https://doi.org/10.1119/1.12419>.